CHEMISTRY OF MATERIALS
Article

Chem. Mater. **2009,** *21,* 3485–3490 3485
DOI:10.1021/cm901362v

Formation and Stability of Ternary Imides in the Li−Mg−N−H Hydrogen Storage System

Jianjiang Hu* and Maximilian Fichtner

Institute for Nanotechnology, Forschungszentrum Karlsruhe, Postfach 3640, D-76021 Karlsruhe, Germany

Received May 18, 2009. Revised Manuscript Received June 19, 2009

The thermodynamic nature of the mixtures consisting of $Mg(NH_2)_2$ and LiH determines the reaction sequence and pathways between the components. That is, the reaction resulting in the formation of $Li_2Mg(NH)_2$ and H_2, which is useful for on-board hydrogen storage, first takes place in the mixtures in spite of various stoichiometries. By varying the molar ratio of $Mg(NH_2)_2$ to LiH in the proximity of 1:2, a maximal amount of H_2 release and low level of ammonia generation were observed for the mixture of $Mg(NH_2)_2$ and LiH at a 1:2 molar ratio. When LiH was in deficit (<2), severe ammonia evolution occurred concomitantly during dehydrogenation. On the other hand, excess in LiH (higher than 2) lowered the hydrogen storage efficiency. In the molar ratio range from 1:1.5 to 1:2.7 of $Mg(NH_2)_2$ to LiH, both dynamic and quasi-equilibrium dehydrogenation resulted in the formation of the ternary imide $Li_2Mg(NH)_2$, indicating the ternary imide is a thermodynamically favored dehydrogenation product in this hydrogen storage system and may explain the cyclic stability of this system.

Introduction

Metal−N−H hydrogen storage systems have attracted considerable attentions in the past few years as alternative hydrogen storage materials to the traditional metal hydrides.[1] Among the systems investigated, Li−Mg−N−H consisting of $Mg(NH_2)_2$ and LiH exhibits reversibility and good hydrogen sorption properties under mild operating conditions.[2−4] A mixture of $LiNH_2$ and MgH_2 is regarded as an equivalent to the $Mg(NH_2)_2$-LiH combination because of the metathesis reaction between the two metal hydride−amide pairs (reaction 1).[4,5]

$$2LiNH_2 + MgH_2 \rightarrow Mg(NH_2)_2 + 2LiH \qquad (1)$$

This conversion can be realized at 220 °C under a hydrogen pressure of 100 bar.[6] Theoretical calculations by density functional theory (DFT) showed that this reaction is an exothermic one with an enthalpy of 68.8 kJ/mol of $Mg(NH_2)_2$ at 0 K.[7] Therefore, after a cycle of hydrogen desorption and rehydrogenation, the $2LiNH_2-MgH_2$ system becomes de facto a $Mg(NH_2)_2$-2LiH system.[8]

Investigations on different stoichiometries of $Mg(NH_2)_2$−LiH were undertaken by different groups for this system in the compositional range from 1:1 to 1:4 of $Mg(NH_2)_2$ to LiH. Various dehydrogenated products were observed, depending on the initial molar ratio of $Mg(NH_2)_2$ to LiH. At 1:1 $Mg(NH_2)_2$−LiH, a ternary imide with the composition of $Li_2Mg_2(NH)_3$ is formed along with large amount of NH_3 generation, which is usually considered unsuitable for hydrogen storage.[9] On the other hand, $Li_2Mg(NH)_2$ is the dehydrogenated product after H_2 release from 1:2 molar ratio in reaction 2.[2,4,5] At 3:8 or 1:2.7 and 1:4 molar ratios (reactions 3 and 4), Mg_3N_2/Li_2NH and Mg_3N_2/Li_3N were identified as desorbed products,[3,10−14] respectively.

$$Mg(NH_2)_2 + 2LiH \rightarrow Li_2Mg(NH)_2 + 2H_2 \quad 5.6\ wt\ \% \qquad (2)$$

$$3Mg(NH_2)_2 + 8LiH \rightarrow 4Li_2NH + Mg_3N_2 + 8H_2 \quad 6.9\ wt\ \% \qquad (3)$$

$$Mg(NH_2)_2 + 4LiH \rightarrow 4Li_3N + Mg_3N_2 + 12H_2 \quad 9.1\ wt\ \% \qquad (4)$$

*Corresponding author. Phone: 49 (0)7247828915. Fax: 49 (0)7247826368. E-mail: jianjiang.hu@kit.edu.

(1) Chen, P.; Xiong, Z. T.; Wu, G. T.; Liu, Y.; Hu, J. J.; Luo, W. F. *Scr. Mater.* **2007**, *56*, 817–822.
(2) Xiong, Z. T.; Wu, G. T.; Hu, J. J.; Chen, P. *Adv. Mater.* **2004**, *16* (17), 1522–1525.
(3) Leng, H. Y.; Ichikawa, T.; Hino, S.; Hanada, N.; Isobe, S.; Fujii, H. *J. Phys. Chem. B* **2004**, *108*, 8763–8765.
(4) Luo, W. *J. Alloys Compd.* **2004**, *381*, 284–287.
(5) Luo, W.; Rönnebro, E. *J. Alloys Compd.* **2005**, *404−406*, 392–395.
(6) Luo, W.; Sickafoose, S. *J. Alloys Compd.* **2006**, *407*, 274–281.
(7) Araújo, C. M.; Scheicher, R. H.; Ahuja, R. *APPL. PHYS. LETTERS* **2008**, *92*, 021907.
(8) Lohstroh, W.; Fichtner, M. *J. Alloys Compd.* **2007**, *446−447*, 332–335.
(9) Xiong, Z. T.; Wu, G. T.; Hu, J. J.; Chen, P.; Luo, W.; Wang, J. *J. Alloys Compd.* **2006**, *417*, 190–194.
(10) Leng, H.; Ichikawa, T.; Fujii, H. *J. Phys. Chem. B* **2006**, *110*, 12964–12968.
(11) Leng, H. Y.; Ichikawa, T.; Hino, S.; Nakagawa, T.; Fujii, H. *J. Phys. Chem. B* **2005**, *109*, 10744–10748.
(12) Aoki, M.; Noritake, T.; Kitahara, G.; Nakamori, Y.; Towata, S.; Orimo, S. *J. Alloys Compd.* **2007**, *428*, 307–311.
(13) Nakamori, Y.; Kitahara, G.; Miwa, K.; Towata, S.; Orimo, S. *Appl. Phys.* **2005**, *A 80*, 1–3.
(14) Nakamori, Y.; Kitahara, G.; Miwa, K.; Ohba, N.; Noritake, T.; Towata, S.; Orimo, S. *J. Alloys Compd.* **2005**, *404−406*, 396–398.

Published on Web 07/14/2009

Higher amounts of hydrogen release were achieved at 3:8 and 1:4 molar ratios as some or all the desorbed compounds are hydrogen-free. However, one must bear in mind that as a material for hydrogen storage the operating temperature has to be considered at the same time. For the molar ratio 3:8, 6.9 wt % hydrogen was measured in the heating process up to 450 °C.[15] Part of the hydrogen capacity can only be obtained by applying higher temperatures, e.g., 500 °C for the 1:4 molar ratio.[15−17] The availability of the hydrogen content at 250 °C in the systems of the three different molar ratios was measured by means of pressure−composition isothermal (PCI) method by Aoki.[17] The dehydrogenation amounts at 250 °C found for the molar ratios of 1:2, 3:8 and 1:4 were 5.4, 5.1, and 4.5 wt %, respectively. The samples with various molar ratios exhibited a same plateau pressure at 250 °C. This strongly suggests that the samples with various stoichiometries were of similar thermodynamic nature. As pointed out by Akbarzadeh et al. recently, it is in general impossible to improve the hydrogen sorption properties simply by adjusting the stoichiometry of the starting materials in the Li−Mg−N−H system, because the chemical pathways for a multicomponent system are tightly constrained by the bulk thermodynamics.[18]

Among the mixtures of different molar ratios, the Li−Mg−N−H system at 1:2 molar ratio possesses high capacity and relatively low operating temperature.[16,17] Recently, Luo et al. reported an encouraging cyclic stability for this composition.[19]

Despite much efforts in the mechanistic and thermodynamic study,[6,11,12,16] different intermediates and therefore controversial postulations concerning the chemical processes in the hydrogen sorption steps were reported, which is in part due to the above-mentioned metathesis reaction. Although emphasis was made on the hydrogen release amount, optimization for the 1:2 molar ratio is lacking. In this study, the compositional optimization on the $Mg(NH_2)_2$−LiH system was made by adjusting the molar ratio of $Mg(NH_2)_2$ to LiH in the proximity of 1:2 to investigate how a deviation from the 1:2 stoichiometry affects the hydrogen sorption performances. The issue concerning the ammonia emission was also addressed.

Experimental Section

Sample Preparation. $Mg(NH_2)_2$ (>95%) was synthesized in-house by heating Mg powder in NH_3 gas at 300 °C. LiH (95%) was purchased from Sigma-Aldrich and used as received without any pretreatment. For the ball-milling process, the starting chemicals were loaded into a milling vessel inside the glovebox with Ar as protecting atmosphere.

Ball milling was conducted on a Retsch PM400 at 200 rpm for 36 h. Samples of $Mg(NH_2)_2-x$LiH mixtures were prepared with the x values (i.e., molar numbers of LiH) equal to 1.5, 1.8, 2.0, 2.2, 2.5, and 2.7, respectively. The milling jar was equipped with a gas valve that can be connected to a pressure gauge and enable the measurement of pressure increase inside the milling jar caused by gas release during ball-milling. To ensure even milling and reduce the heat effects arising from milling, we set the mill to revolve for 60 s in one direction, pause 15 s, and then revolve in the reverse direction. No obvious temperature increase was noticed, thanks to the ventilation device inside the compartment of the mill.

Characterization Methods. The tests of temperature-programmed desorption (TPD) coupled with a mass spectrometer from Hiden Analysis were carried out on a home-built apparatus. About 100 mg of sample was loaded into a tube reactor housed in a tubing furnace. Purified Ar was used as purge gas, which flowed into a thermal conductivity detector. The evolution of H_2 from samples by heating induces an increase in thermal conductivity that was recorded. Simultaneous monitoring of NH_3 generated from the dehydrogenation was then realized by the mass spectra. The heating rate was kept at 2 °C/min for all tests. The volumetric desorption measurements were performed on a commercial Sieverts' gas reaction system. About 300 mg of the mixture was used in each experiment. The measurement was conducted in an automatic release mode, during which the whole system was first evacuated. The hydrogen was released into the vacuum. The reactor was heated at the same ramping rate as in TPD tests (2 °C/min). The measurements of Fourier Transform Infrared Spectroscopy (FTIR) were conducted on a Perkin Elemer FTIR-3000 Spectrometer at a resolution of 4 cm^{-1}. For the X-ray diffractometry (XRD) measurements (Bruker D8-advance X-ray diffractometer with Cu Kα radiation), about 50 - 70 mg of sample was pressed into pellets and fixed to the XRD sample holder which was housed inside a Kapton hood. Differential scanning calorimetry (DSC) measurements were performed on a Netzsch DSC 204 HP housed inside the glovebox. Samples were heated at 2 °C/min under the flow of purified Ar at 30 mL/min. For the determination of NH_3 amount generated during ball milling, the gaseous products were slowly introduced from the milling jar to distilled water through a filter so that NH_3 was absorbed upon contacting with water. Similarly, the gases from the exit of TPD experiments were subjected to flow through distilled water to collect NH_3 evolving from the TPD tests. The quantitative determination of ammonia was then conducted on a Metrohm 781 pH/Ion Meter (Switzerland) equipped with an NH_3-selective electrode. The measuring range of the model is $0.1-1.7 \times 10^4$ ppm (NH_3). Aqueous solutions with known concentrations of NH_4Cl were used for the calibration. A detailed description is given in ref 20.

Results and Discussion

The conditions applied in mechanochemical alloying have profound effects on the subsequent solid-state reactions. Insufficient ball milling may lead to large extent of side-reactions. On the other hand, mechanochemical ball-milling can cause local pressure rise to several GPa,[21] and

(15) Ichikawa, T.; Tokoyoda, K.; Leng, H.; Fujii, H. *J. Alloys Compd.* **2005**, *400*, 245–248.
(16) Janot, R.; Eymery, J.-B.; Tarascon, J.-M. *J. Power Sources* **2007**, *164*(2), 496–502.
(17) Aoki, M.; Noritake, T.; Nakamori, Y.; Towata, S.; Orimo, S. *J. Alloys Compd.* **2007**, *446−447*, 328–331.
(18) Akbarzadeh, A. R.; Ozoliņš, V.; Wolverton, C. *Adv. Mater.* **2007**, *19*(20), 3233–39.
(19) Luo, W.; Wang, J.; Stewart, K.; Clift, M.; Gross, K. *J. Alloys Compd.* **2007**, *446−447*, 336–341.
(20) Liu, Y. F.; Hu, J. J.; Wu, G. T.; Xiong, Z. T.; Chen, P. *J. Phys. Chem. C* **2008**, *112*, 1293–1298.
(21) Balema, V. P.; Balema, L. *Phys. Chem. Chem. Phys.* **2005**, *7*, 1310–1314.

Table 1. NH_3 Emission and Gravimetric Hydrogen Release of the Investigated Compositions

X value	NH_3 concentration in ball milling step (ppm)	NH_3 concentration in TPD test (ppm)	H atoms released in ball milling step[a]	H atoms released in volumetric method	H atoms released Total	total H release (wt %)
1.5			0.48	2.52	3.00	4.4
1.8	1866	6684	0.42	3.10	3.52	5.0
2.0	317	516	0.43	3.24	3.67	5.1
2.2	370	406	0.29	3.39	3.68	5.0
2.5	294	239	0.30	3.34	3.64	4.8
2.7	217	275	0.31	3.41	3.72	4.8

[a] Calculated from the pressure increase in the milling vessel via the gas equation.

thus reactions may take place during the ball-milling process. For example, the mixtures of $Mg(NH_2)_2$ and MgH_2 exhibited thermal decomposition behavior of the individual components for insufficiently ball milled mixtures, i.e., $Mg(NH_2)_2$ decomposes first to MgNH and NH_3 followed by the dehydrogenation of MgH_2. In contrast, H_2 evolution from the reaction between $Mg(NH_2)_2$ and MgH_2 took place under certain ball milling conditions.[22,23] Therefore, a proper selection of milling energy and milling duration is often needed.

Under the ball milling conditions in the current study, a slight generation of gaseous products was observed by measuring the pressure inside the milling jar after ball-milling. Table 1 lists the H_2 amount released during ball milling. It seems that more hydrogen was evolved at lower x values. Because of the composition variation, the ball to powder weight ratio changed from 35 at $x = 1.5$ to 31 at $x = 2.7$, although the same parameters were used. We believe the higher ball to powder weight ratio was responsible for the relatively higher amount in the gas generation in the ball milling step. The hydrogen evolution in the TPD tests was not very much pronounced by the stoichiometric relationship between $Mg(NH_2)_2$ and LiH (Figure 1). The peak temperature of the main hydrogen desorption shifted slightly to lower temperature with increased LiH content. Nevertheless, tailing in the hydrogen desorption became more apparent as the LiH content increases, which was attributed to the stability of the transitory imide phases.[16]

NH_3 generation poses a serious issue for the metal−N−H hydrogen storage systems, because a substantial part of hydrogen are bonded with N atoms. Therefore, the loss of N-content in terms of NH_3 release means the loss of hydrogen capacity. Moreover, the changes in stoichiometry caused by the NH_3 emission lead to the material deterioration and lower the hydrogen sorption performances. NH_3 is also poisonous to the catalysts in the fuel cell of proton exchange membrane (PEM).[24,25] Even at a concentration of 1 ppm, NH_3 can significantly lower the performance of the fuel cell.[26] This problem has to be tackled prior to the practical application.

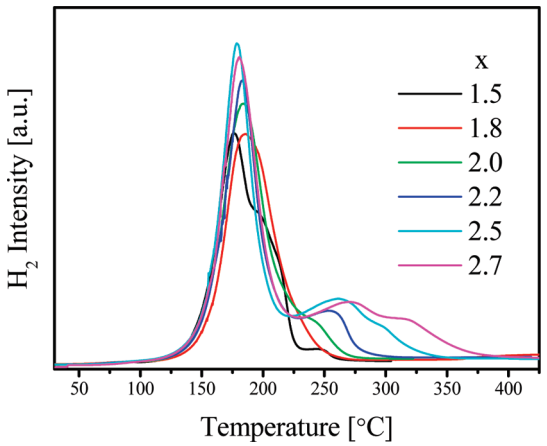

Figure 1. TPD curves of samples from $x = 1.5$ to 2.7.

The estimation of NH_3 emission was previously developed by Hino et al. using Raman spectroscopy for the $LiNH_2$−2LiH system.[27] Later on they applied infrared spectroscopy to quantify NH_3 amount[28] in the desorbed gas. 0.1% or 1000 ppm NH_3 was calculated in the desorbed H_2 gas until 400 °C from the $LiNH_2$−2LiH system. Luo and Steward reported a novel method to determine the NH_3 in the desorbed H_2 from Li−Mg−N−H system using a commercial product called Draeger Tube which has been used in the petroleum refinery industry for decades to detect the impurity.[29] The accuracy was reported to be ±15%. They found that the NH_3 evolution is related to the desorption temperature: from 180 ppm at 180 °C to 720 ppm at 240 °C. Using the same device as in the present study, the temperature dependence of NH_3 concentration at equilibrium was also observed by Liu et al.[20] The ammonia concentration doubled from 250 ppm at 165 °C to 500 ppm at 200 °C.

In contrast to the behavior in hydrogen desorption, ammonia generation was strongly affected by the molar ratio of $Mg(NH_2)_2$ to LiH (Table 1 and Figure 2). The amounts of NH_3 generation in the TPD experiments were low around 175 °C for the samples with x from 2.0 to 2.7. For the sample at $x = 1.5$, severe ammonia evolution was observed just above 200 °C in addition to the concomitant emission with H_2 release at 175 °C. Over 10 times amount of ammonia was measured as compared to those with $x \geq 2.0$ (Table 1). At $x = 1.8$, there were three peaks of

(22) Nakamori, Y.; Kitahara, G.; Orimo, S. *J. Power Sources* **2004**, *138*, 309–312.
(23) Hu, J. J.; Xiong, Z.; Wu, G.; Chen, P.; Murata, K.; Sakata, K. *J Power Sources* **2006**, *159*, 120–125.
(24) Rajalakshmi, N.; Jayanth, T.; Dhathathreyan, K. *Fuel Cells* **2003**, *3*, 177–180.
(25) Uribe, F; Gottesfeld, S.; Zawodzinski, T.Jr. *J. Electrochem. Soc.* **2002**, *149*, A293–A296.
(26) Halseid, R.; Vie, P. J. S.; Tunold, R. *J. Power Sources* **2006**, *154*, 343–350.
(27) Hino, S.; Ichikawa, T.; Ogita, N.; Udagawa, M.; Fujii, H. *Chem. Commun.* **2005**, 3038–3040.
(28) Hino, S.; Ichikawa, T.; Tokoyoda, K.; Kojima, Y.; Fujii, H. *J. Alloys Compd.* **2007**, *446*−*447*, 342–344.
(29) Luo, W.; Stewart, K. *J. Alloys Compd.* **2007**, *440*, 357–361.

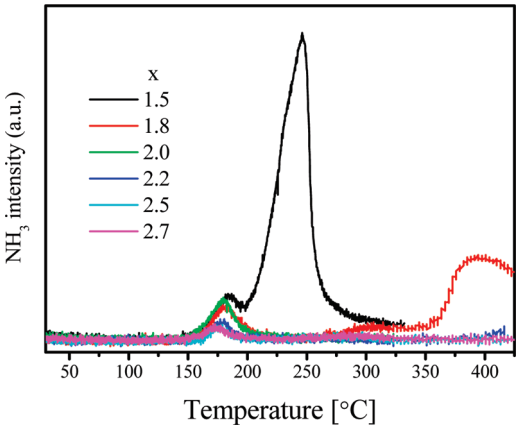

Figure 2. Simultaneous TPD-MS of NH_3 monitoring.

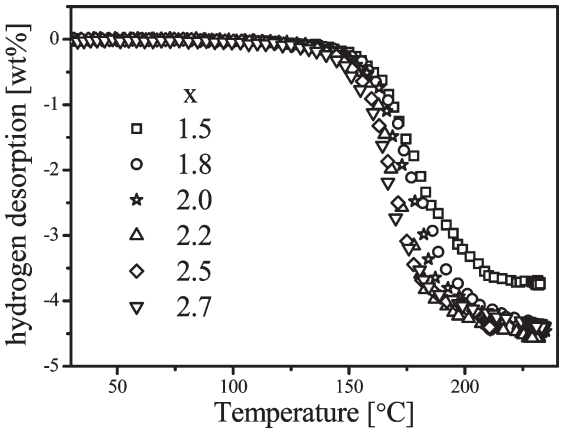

Figure 3. Volumetric determination of H_2 desorption amount at 2 °C/min temperature ramping.

ammonia evolution at 175 °C, 300 °C and 380 °C, respectively (Figure 2). Compared to the ammonia values obtained by the Draeger tube in ref 29 for $Mg(NH_2)_2-2LiH$ (i.e., $x = 2$ in this paper), our results correspond to their ammonia concentration desorbed between 210 and 220 °C. Although the TPD tests were conducted to 400 °C, as can be seen in Figure 2, the generation of ammonia almost completed below 220 °C for the samples with $x \geq 2$. The coincidence in the ammonia values from both methods implies that the method used in the present study has a precision that is comparable to the Draeger tube and thus higher than the spectroscopic approach.

NH_3 concentration during ball-milling was found to be at a similar level of about 300 ppm when the x value was equal or above 2 (Table 1). However, for $x = 1.8$, just below 2.0, a much higher level of NH_3 was detected (about 1870 ppm). Magnesium amide begins to decompose to ammonia upon heating at temperatures above 200 °C in ref 3, although it was recently reported at 300 °C by Liu et al. in ref 20. For $x \geq 2$, the generation of H_2 along with NH_3 in the ball-milling jar is presumably attributed to the dehydrogenation reactions caused by inhomogeneously local heating from ball-milling, taking into account of the similar NH_3 levels measured with TPD exit gas for the same molar ratio. Although solely ball-milling magnesium amide resulted in amorphous substance[30] and no pressure increase was detected, the decomposition of $Mg(NH_2)_2$ due to ball-milling could not be excluded.

The abrupt decrease in NH_3 emission at $x = 2$ indicates that $x = 2.0$ (i.e., $Mg(NH_2)_2-2LiH$) is a threshold value, below which ammonia generation occurs substantially. For $x = 2.0$, the ratio of the $H^{\delta+}$ atoms in the amide to the $H^{\delta-}$ atoms in the hydride is 2:1, indicating that only half of the $H^{\delta+}$ atoms was converted to hydrogen gas in the low temperature range, which led to the formation of imide groups, in this case $Li_2Mg(NH)_2$ [2]. Thus, excessive amide ($x < 2.0$) was responsible for the higher ammonia levels both in the ball-milling step and in the TPD tests. On the contrary, very low level of NH_3 generation was found at $x = 4$ with a large excess of LiH in the composition, as reported by Aoki et al.,[17] which can be interpreted by the extreme reaction readiness of LiH with NH_3.[31]

The quantitative measurements on the hydrogen release amount were conducted in the temperature range of 25−230 °C for all samples. The same trend was observed as in the TPD measurements in terms of hydrogen desorption temperature (Figure 3). With increased LiH content, the onset dehydrogenation temperatures shifted slightly to the lower position.

In a volumetric measurement, the instrument measures the pressure increase exerted by gaseous products. The amount of gases is calculated by applying gas equation with some correction to ideal gas. In the determination of hydrogen desorption, because the molecular weight of NH_3 is 8.5 times that of hydrogen molecule, i.e., with the same weight of gas H_2 generates a pressure 8.5 times high as NH_3 does. The partial pressure generated by NH_3 is very low compared to the partial pressure of H_2. So the contribution from hydrogen is much higher than from NH_3 and therefore the deviation from NH_3 emission is still low for samples with $x < 2$. Together with the H_2 evolved in the milling step, the total desorbed hydrogen amount varied from about 4.4 to 5.1 wt % as shown in Table 1. The sample at $x = 2.0$ peaked the hydrogen desorption amount (Figure 4), indicating the favorable stoichiometry for hydrogen capacity of the amide and hydride pair. For the samples of $x \geq 2.0$, a steady number of H atoms of about 3.7 was observed, close to the theoretical value of 4, which supports the assumption that hydrogen releasing reaction can not proceed beyond reaction 2 in the low-temperature range (below 250 °C).

The thermal effects during the primary dehydrogenation process remained endothermic for all the samples, as shown in the DSC results (Figure 5). The endothermic events at higher temperature could be accounted for by the reaction between the product of the primary dehydrogenation i.e. $Li_2Mg(NH)_2$ and the excessive LiH for the samples with higher x values.[16] For the samples of $x = 1.5$ and 1.8 with LiH in deficit, the decomposition reaction of the excessive $Mg(NH_2)_2$ to MgNH may take place accompanied by the evolution of NH_3.

(30) Hu, J. J.; Wu, G.; Liu, Y.; Xiong, Z.; Chen, P. *J. Phys. Chem. B* **2006**, *110*, 14688–14692.

(31) Hu, Y. H.; Ruckenstein, E. *J. Phys. Chem. A* **2003**, *107*, 9737–9739.

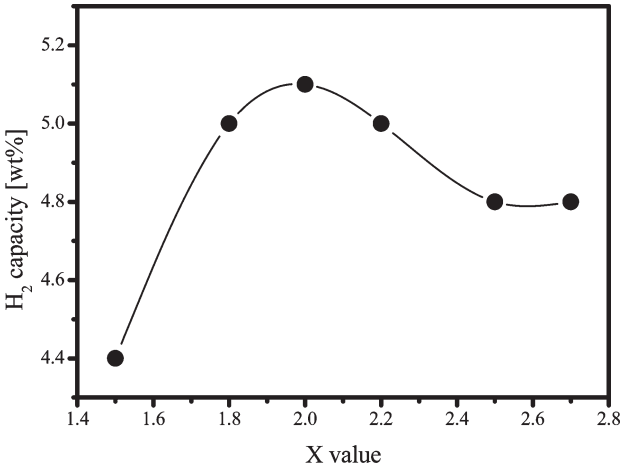

Figure 4. Hydrogen capacity in relationship to x value.

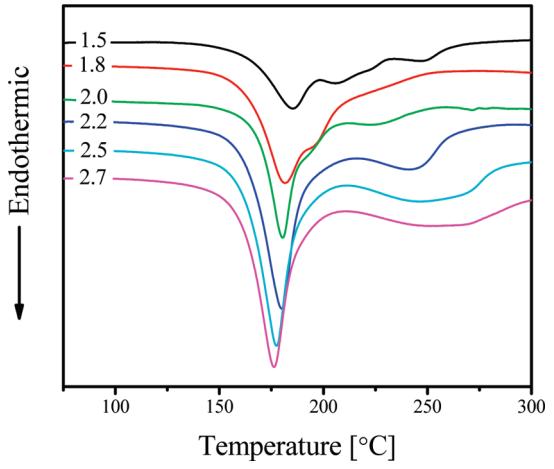

Figure 5. DSC measurements of samples from $x = 1.5$ to 2.7.

Compared to the strong compositional dependence of the ammonia generation and dehydrogenation, the phase development during the TPD measurements and volumetric measurements seems less responsive to the amide/hydride molar ratio. For samples prepared by TPD tests until 250 °C, the cubic $Li_2Mg(NH)_2$ was observed (Figure 6), whereas those samples from volumetric release appeared to be orthorhombic (Figure 7). As reported in the previous work,[32,33] a cubic or orthorhombic structure could result, respectively, depending on the dehydrogenation conditions. Rijssenbeek et al. investigated systematically the formation of the different crystal structures of $Li_2Mg(NH)_2$ by means of combined synchrotron in situ X-ray diffraction and neutron diffraction. The orthorhombic $Li_2Mg(NH)_2$ (α-phase) can only be regenerated by cycling under hydrogen pressure which is converted to a primitive cubic phase (β-$Li_2Mg(NH)_2$) at about 350 °C and then to a face-centered cubic phase (γ-$Li_2Mg(NH)_2$) at 500 °C.[34] In this study, the samples obtained after TPD tests with purging Ar showed the cubic crystal structure,

(32) Hu, J. J.; Liu, Y.; Wu, G.; Xiong, Z.; Chen, P. *J. Phys. Chem. C* **2007**, *111*, 18439–18443.
(33) Yang, J.; Sudik, A.; Wolverton, C. *J. Alloys Compd.* **2007**, *430*, 334–338.
(34) Rijssenbeek, J.; Gao, Y.; Hanson, J.; Huang, Q.; Jones, C.; Toby, B. *J. Alloys Compd.* **2008**, *454*, 233–244.

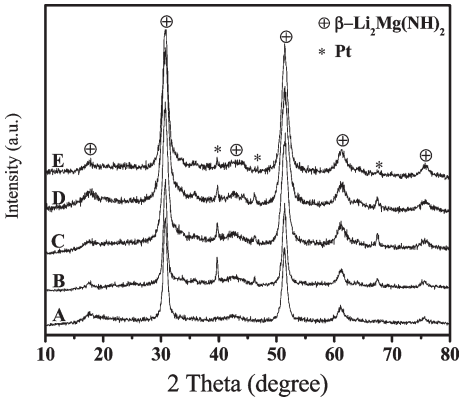

Figure 6. XRD profiles obtained from samples subjected to TPD tests (from A−E $x = 1.8$, 2.0, 2.2, 2.5, 2.7; Pt was from sample holder).

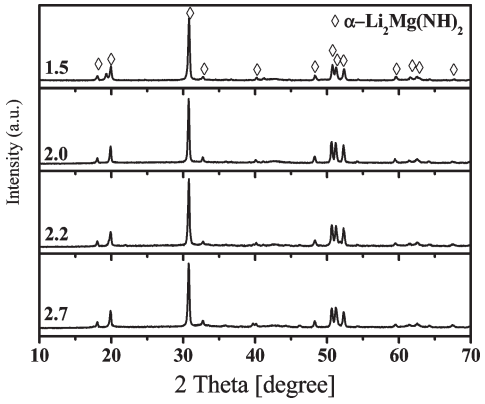

Figure 7. XRD profiles obtained from samples subjected to volumetric release tests.

whereas the orthorhombic phase was observed for the samples after the volumetric measurements, whereby a backpressure was formed from the accumulated H_2 gas. This strongly suggests that the ternary imide $Li_2Mg(NH)_2$ is the most stable one among the reported intermediate ternaries.[6,12] The stoichiometric deviation from the 1:2 molar ratio could be leveled off by NH_3 emission when $x < 2.0$. N−H vibrations were detected in the FTIR measurements, showing strong broad peaks centered at about 3175 cm^{-1} in Figure 8, which is the characteristic absorbance of N−H of the ternary imide $Li_2Mg(NH)_2$, consistent with the XRD analysis. Additional two peaks at 3258 and 3312 cm^{-1} present in the sample of $x = 1.5$ indicates that $LiNH_2$ was formed after the dehydrogenation. $LiNH_2$ can be generated from the metathesis reaction (Reaction 1) reported by Luo et al. [5]. In case of $x = 1.5$, the NH_2 groups were in excess according to reaction 2.

According to the findings reported in ref 32, the hydrogen sorption process of the Li−Mg−N−H system consists of two steps

$$2Li_2Mg(NH)_2 + H_2 \leftrightarrow LiH + LiNH_2 + Li_2Mg_2(NH)_3 \quad (5)$$

in the slope region and

$$LiNH_2 + Li_2Mg_2(NH)_3 + 3H_2 \leftrightarrow 3LiH + 2Mg(NH_2)_2 \quad (6)$$

in the plateau region. The equilibrium pressure of the plateau at 220 °C was first reported by Luo to be 41 bar.[5]

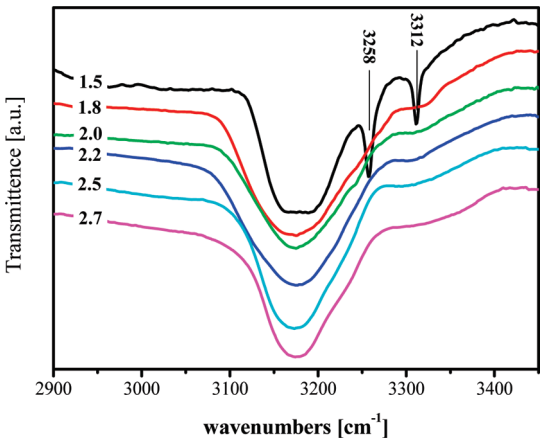

Figure 8. FTIR spectra of dehydrogenated samples.

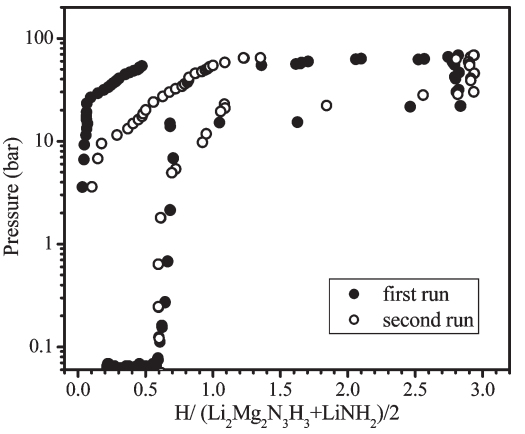

Figure 9. PCI measurements of the sample $Li_2Mg_2(NH)_3-LiNH_2$.

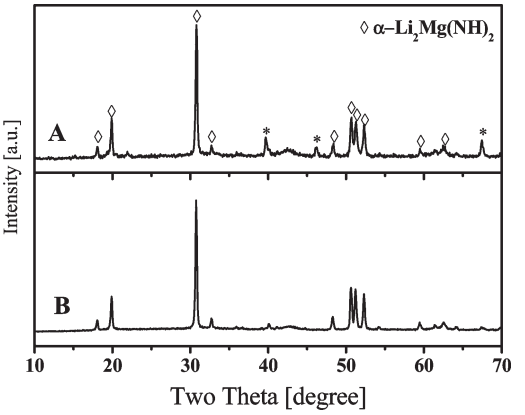

Figure 10. XRD profiles of the sample $Li_2Mg_2(NH)_3-LiNH_2$ after PCI measurement (A) and α-$Li_2Mg(NH)_2$ for reference (B) (the peaks labeled with * were caused by Pt of the sample holder).

By measuring isotherms at different temperatures, the van't Hoff plot was drawn, from which the enthalpy change of dehydrogenation was calculated from the slope to be 39 kJ/mol of H_2.[5,35] Extrapolating the van't Hoff plot to 1 bar pressure, the temperature obtained was about 90 °C, which is close to the operating temperature of a PEM fuel cell. In addition, this reaction can deliver 4.2 wt % hydrogen. It would be interesting to know whether hydrogen sorption could be reversibly realized via reaction 6 independently. Therefore, $Li_2Mg_2(NH)_3$ was specially synthesized according to ref[32] and mixed with $LiNH_2$ at 1:1 molar ratio. To compare to the previous results, we chose 220 °C for the isotherm. Shown in Figure 8 were the PCI results of the $Li_2Mg_2(NH)_3$:$LiNH_2$ mixture at 220 °C. A shortened slope and accordingly a longer plateau compared to that from the pristine 1:2 $Mg(NH_2)_2-LiH$ system were indeed observed in the first run, as expected (Figure 9). The hydrogenation reached a value close to the stoichiometric 3 H atoms as described in reaction 6 from 1/2[$Li_2Mg_2(NH)_3-LiNH_2$] as well. Compared to the $Mg(NH_2)_2-LiH$ (1:2) system,[35] the equilibrium pressure remained unchanged. However, a long absorption slope appeared during the second run, resembling the neat $Mg(NH_2)_2-2LiH$ system. The XRD analysis of the post-PCI sample (Figure 10) manifested that only the typical diffractions originated from the orthorhombic ternary imide $Li_2Mg(NH)_2$ appeared instead of the starting components, i.e., $LiNH_2$ and $Li_2Mg_2(NH)_3$. Re-examining reaction 6, we found that $Mg(NH_2)_2$ and LiH will be formed after PCI absorption albeit at 1:1.5 molar ratio. Although the subsequent dehydrogenation was conducted under quasiequilibrium in contrast to the dynamic dehydrogenation in the above sections (both TPD and volumetric release), the stable ternary imide $Li_2Mg(NH)_2$ was still resulted. The stability of $Li_2Mg(NH)_2$ could be a factor for the cyclic stability of the Li−Mg−N−H system.

Conclusions

By varying the molar ratio of $Mg(NH_2)_2$ and LiH, an optimal composition of $Mg(NH_2)-2LiH$ was found for this hydrogen storage system in terms of hydrogen capacity and ammonia generation. Deviation from this composition leads to the inefficiency of hydrogen storage or ammonia emission. Both dynamic and quasiequilibrium dehydrogenation resulted in the formation of the ternary imide $Li_2Mg(NH)_2$, which may be a reason for the good cycle stability.

Acknowledgment. The authors thank the EU-Project "NanoHy" (Contract 210092) for financial support.

(35) Xiong, Z. T.; Hu, J. J.; Wu, G. T.; Chen, P.; Luo, W. F.; Gross, K.; Wang, J. *J. Alloys Compd.* **2005**, *398*(1−2), 235–239.